Vibrational–Translational Energy Transfer in the Near-Adiabatic Approximation*

MARY ATTERMEYER AND R. A. MARCUS
Noyes Chemical Laboratory, University of Illinois, Urbana, Illinois 61801
(Received 31 March 1969)

Vibrational–translational energy transfer is examined in the near-adiabatic (or perturbed stationary states) approximation. The results are classical, and the method used is related to that of Marcus [J. Chem. Phys. **49**, 2617 (1968)]. The results are compared with those of the more usual ("static") approximation and with the exact results. The PSS results were good at low energies at all mass ratios studied, unlike the static results. For certain mass ratios the static approximation fails badly, even at very low transition probabilities. For other mass ratios, the results are of comparable accuracy except at high energies where the static one is somewhat better. Reasons for the above behavior are discussed, and implications regarding existing infinite-order distorted wave and semiclassical calculations are noted. The relation to a recent correction of the Jackson–Mott calculation is described.

INTRODUCTION

For the most part the theoretical treatment of vibrational–translational energy transfer[1–7] in a molecular collision has been given in terms of a "static" (ST) approximation. The ST treatment has been quantum,[2] semiclassical,[3,4] or classical.[5] A principal ST feature lies in its zeroth-order approximation—an elastic collision in which the vibrational motion is that of an isolated molecule and in which the effective potential energy of relative translational motion is uninfluenced by the vibrational motion. A comparison[7] of the exact classical numerical results with those of the classical ST approximation shows that it is excellent for certain mass ratios but that it fails badly for others even when a classical analog of the transition probability is extremely small.

An alternative zeroth-order approximation is that of perturbed stationary states (PSS),[8] which can also be described as the adiabatic approximation. According to the PSS approximation the zeroth-order (elastic) collision is one in which the vibrational motion is allowed to be distorted during the encounter and in which the relative motion is perturbed accordingly.[9,10] The desirability of having such an approximation available is evident upon examination of a trajectory under conditions where the ST approximation failed, e.g., in Fig. 5 of Ref. 7 there is a large *transient* distortion of the oscillator coordinate during the collision.

Previous PSS calculations do not appear to have been made for vibrational–translational energy transfer. The classical PSS approximation is explored in the present paper and compared with the exact results of Kelley and Wolfsberg[7] and Secrest.[11,12] Because of correspondence arguments[13] it may be anticipated that findings of the present study regarding the relative merits of ST and PSS approximations will be applicable to the quantum and semiclassical cases also, thereby yielding various predictions for these cases as described later.

A theoretical treatment analogous to that in Ref. 9(c) is used below. A corresponding quantum treatment is given in Ref. 9(a).

THEORY

For a collinear collision between an atom A and a harmonic oscillator BC, let x denote the coordinate of

* Acknowledgement is made to the National Science Foundation and to the donors of the Petroleum Research Fund, administered by the American Chemical Society, for the support of this research.

[1] E.g., Recent reviews: (a) K. Takayanagi, Progr. Theoret. Phys. (Kyoto), Suppl. **25**, 1 (1963); (b) K. Takayanagi, Advan. At. Mol. Phys. **1**, 149 (1965); (c) D. Rapp and T. Kassal, Chem. Rev. **69**, 61 (1969).

[2] E.g., (a) C. Zener, Phys. Rev. **37**, 556 (1931); J. M. Jackson and N. F. Mott, Proc. Roy. Soc. (London) **A137**, 703 (1932); O. K. Rice, J. Am. Chem. Soc. **54**, 4558 (1932); R. N. Schwartz, Z. I. Slawsky, and K. F. Herzfeld, J. Chem. Phys. **20**, 1591 (1952); K. F. Herzfeld and T. A. Litovitz, *Absorption and Dispersion of Ultrasonic Waves* (Academic Press Inc., New York, 1959); D. Rapp, J. Chem. Phys. **40**, 2813 (1964); B. Hartmann and Z. I. Slawsky, *ibid.* **47**, 2491 (1967); S. L. Thompson, *ibid.* **49**, 3400 (1968); (b) J. H. Weare and E. Thiele, *ibid.* **48**, 513 (1968); E. Thiele and J. Weare, *ibid.* **48**, 2324 (1968).

[3] E.g., First order: C. Zener, Proc. Cambridge Phil. Soc. **29**, 136 (1932); E. Bauer, J. Chem. Phys. **23**, 1087 (1955); J. B. Calvert and R. C. Amme, *ibid.* **45**, 4710 (1966).

[4] E.g. Infinite order: E. Kerner, Can. J. Phys. **36**, 371 (1958); C. E. Treanor, J. Chem. Phys. **43**, 532 (1965). [Independent solutions of the linear forced oscillator time-dependent Schrödinger equation are given in M. S. Bartlett and J. E. Moyal, Proc. Cambridge Phil. Soc. **45**, 545 (1949); R. P. Feynmann, Phys. Rev. **84**, 108 (1951); G. Ludwig, *Die Grundlagen der Quantenmechanik* (Springer-Verlag, Berlin, 1954), Chap. 1; L. C. Biedenbarn and P. J. Brussard, *Coulombic Excitation* (Clarendon Press, Oxford, England, 1965), Chap. 5]; T. E. Sharp and D. E. Rapp, J. Chem. Phys. **43**, 1233 (1965); C. E. Treanor, *ibid.* **44**, 2220 (1966).

[5] (a) L. Landau and E. Teller, Physik. Z. Sowjetunion **10**, 34 (1936); (b) J. G. Parker, Phys. Fluids **2**, 449 (1959); D. Rapp, J. Chem. Phys. **32**, 735 (1960); K. Takayanagi, Ref. 1(a); D. Rapp, Ref. 2(a).

[6] F. H. Mies, J. Chem. Phys. **40**, 523 (1964); **41**, 903 (1964).

[7] J. D. Kelley and M. Wolfsberg, J. Chem. Phys. **44**, 324 (1966).

[8] N. F. Mott and H. S. W. Massey, *The Theory of Atomic Collisions* (Clarendon Press, Oxford, England 1965), 3rd ed.; K. F. Herzfeld and T. A. Litovitz, Ref. 2; K. Takayanagi, Ref. 1(b).

[9] (a) R. A. Marcus, J. Chem. Phys. **45**, 4493 (1966) (Pt. I); (b) **45**, 4500 (1966) (Pt. II); (c) **49**, 2617 (1968) (Pt. IV). In Eq. (93) of Pt. IV the $2J_\rho^0)^{1/2}$ should read $2(J_\rho^0)^{1/2}$.

[10] R. D. Levine, J. Chem. Phys. **49**, 51 (1968).

[11] D. Secrest, J. Chem. Phys. **51**, 421 (1969).

[12] Other highly useful exact classical calculations (Benson and co-workers) are reviewed in Ref. 1(c).

[13] Compare R. A. Marcus, J. Chem. Phys. (to be published).

TABLE I. Comparison of exact and approximate vibrational energy transfers.

$C-B+A$	E_0	μ	ΔE	$\Delta E^{PSS}/\Delta E$	$\Delta E^{ST}/\Delta E$	KW Case no.
1−12+1	0.00929	12.96	8.38×10^{-5}	1.01	1.01	I-2
1−12+13	0.00232	4.899	8.62×10^{-10}	1.00	1.07	II-5b
	0.00929		1.05×10^{-5}	1.01	1.07	I-5b
	0.0739		0.00494	1.05	1.06	I-5d
12−12+2	0.195	3.606	0.0290	1.15	1.12	IV-24[b]
	0.393		0.0781	1.29	1.13	I-7b
	0.781		0.180	1.55	1.14	II-7d
	3.12		0.800	2.76	1.15	I-7d
12−12+24	0.195	1.414	0.00691	1.16	2.34	II-13c
	0.393		0.00570	1.28	2.33	I-13b
	0.781		0.261	1.47	2.29	II-13d
	3.12		2.18	2.24	2.22	I-13d
1−1+24	0.0981	1.041	1.55×10^{-5}	1.10	5.26	IV-10
	0.195		8.00×10^{-4}	1.19	5.38	IV-27
	0.393		0.0134	1.34	5.60	I-18b
	0.781		0.0914	1.65	5.98	I-18c
12−1+13	0.334	0.4082	1.51×10^{-8}	1.09[a]	1260	II-26b
	0.666		2.75×10^{-6}	1.35[a]	1670	IV-39
	1.34		6.11×10^{-5}	2.34	3810	I-26b
	2.66		6.29×10^{-6}	116	574,000	IV-37

[a] ΔE^{PSS} computed by method of Ref. 16(b).
[b] The numeral following "IV" indicates the line of data in Table IV of Ref. 7 to which this calculation refers.

relative translational motion

$$[x=r_A-(m_Br_B+m_Cr_C)/(m_B+m_C)]$$

and y denote the oscillator displacement from its equilibrium bond length r_e ($y=r_B-r_C-r_e$). The Hamiltonian H is

$$H=\tfrac{1}{2}[(p_x^2/M)+(p_y^2/m)+m\omega_0^2y^2]+V(x,y), \quad (1)$$

where M and m are the reduced masses,

$$m_A(m_B+m_C)/(m_A+m_B+m_C)$$

and

$$m_Bm_C/(m_B+m_C),$$

$\omega_0/2\pi$ is the oscillator vibrational frequency, and $V(x, y)$ is the interaction potential[14]; p_x and p_y are the momenta conjugate to x and y.

In the particular case that V has an exponential dependence on the r_{AB} distance, r_A-r_B,

$$V(x,y)=D\exp(-br_{AB})=D\exp[-b(x-\lambda y-\lambda r_e)], \quad (2)$$

where λ is $m_C/(m_B+m_C)$ and b^{-1} is an effective range parameter, dimensionless quantities v, z, and $\tilde{H}$ can be introduced[11]:

$$\tilde{H}=\tfrac{1}{2}(p_z^2+p_v^2+v^2)+\exp(v-\mu z), \quad (3)$$

where $\tilde{H}$ is $H(b\lambda/m^{1/2}\omega_0)^2$, v is $b\lambda y$, z is

$$[b(x-\lambda r_e)-\ln(Db^2\lambda^2/m\omega_0^2)]/\mu, \quad (4)$$

p_v and p_z are $dv/d(\omega_0t)$ and $dz/d(\omega_0t)$, and μ is[15]

$$\mu=[m_B(m_A+m_B+m_C)/m_Am_C]^{1/2}. \quad (5)$$

When the rectilinear coordinates v and z are employed, the local adiabatic vibrational potential U is obtained by expanding the last two terms of (3) in a power series about the value of v, v_e, which minimizes U (at each z):

$$U(v,z)=U(v_e,z)+\tfrac{1}{2}\omega^2(v-v_e)^2+\cdots, \quad (6)$$

where v_e satisfies (7):

$$\partial[\tfrac{1}{2}v^2+\exp(v-\mu z)]/\partial v=0 \qquad (\text{at } v=v_e), \quad (7)$$

and where ω^2 is $\partial^2U/\partial v^2$ at $v=v_e$. One then finds

$$v_e=-\exp(v_e-\mu z), \quad (8)$$

$$U(v_e,z)=\tfrac{1}{2}v_e^2-v_e, \quad (9)$$

$$\omega^2=1-v_e. \quad (10)$$

Comparison of (6) with the expansion in Ref. 9(c) leading to Eqs. (79) and (80) shows that use can be made of the arguments employed there to derive (91) to (94), but with ρ, ρ_0, and μ there replaced by v, v_e, and 1 here. When the $\dot{\omega}$ term in (91) is neglected one obtains (93), which yields (11). For completeness, the derivation of (11) is also outlined in the Appendix of the present paper, and an $\dot{\omega}$ term is given by (A8)

[14] Use of an anharmonic oscillator potential in (1) would offer no added calculational difficulty if the local harmonic expansion in Eq. (7) continued to be valid. Otherwise the treatment could be modified by adapting certain methods from nonlinear mechanics (for example, making the local oscillator approximately a harmonic one but with an amplitude-dependent frequency) or using the numerical method noted in Ref. 16(b).

[15] μ^2 equals the quotient $4/\lim(\Delta E_{av}/E_0)$, whose denominator is discussed in Kelley and Wolfsberg.[7]

there;

$$J(\tau)=J^0-2(J^0)^{1/2}\int_{-\infty}^{\tau}\dot{v}_e(\omega\pi)^{1/2}\times\sin\left[\int_{\tau_0}^{\tau'}\omega(\tau'')\,d\tau''+\delta\right]d\tau'+\left|\int_{-\infty}^{\tau}\dot{v}_e(\omega\pi)^{1/2}\exp\left[i\int_{\tau'}^{\tau}\omega(\tau'')\,d\tau''\right]d\tau'\right|^2, \quad (11)$$

where $J(\tau)$ is the vibrational action of the $(v-v_e)$ oscillator at reduced time τ, $(\tau=\omega_0 t)$, J^0 is its initial value, and δ is a vibrational phase at some specified time τ_0 before the interaction has occurred.

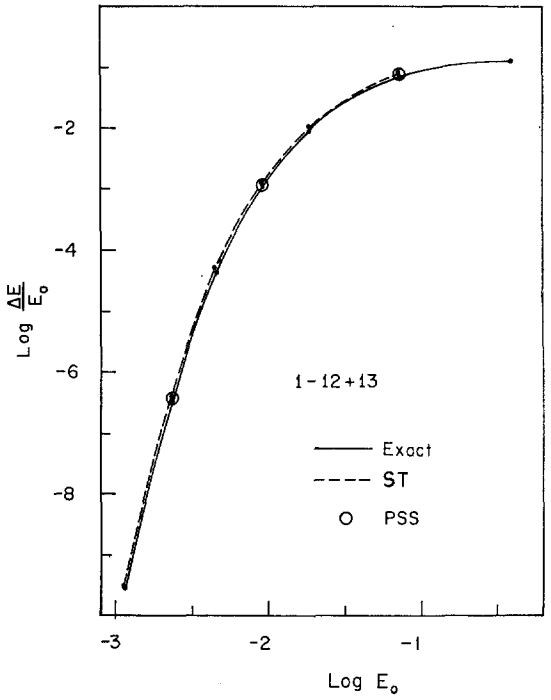

FIG. 1. Log $\Delta E/E_0$ vs log E_0 for a $1-12+13$ collision. The exact results are taken from Ref. 7, apart from the log $E_0=-0.41$ point.[16]

The origin for τ can be chosen without loss of generality to be the time when z attains its minimum value. As τ tends to $\pm\infty$, ω tends to unity. Thus, the local vibrational energy, $J\omega/2\pi$, becomes $J^0/2\pi$ at $\tau=-\infty$ and $J^\infty/2\pi$ at $\tau=+\infty$. The vibrational-energy change in units of $m(\omega_0/b\lambda)^2$ is

$$\Delta E_{\text{vib}}=(J^\infty-J^0)/2\pi. \quad (12)$$

RESULTS

Comparison of values obtained for Eq. (12) is made with those from the exact numerical integration of Kelley and Wolfsberg[7] and with those given by the classical (ST) expression of Parker, Takayanagi, and Rapp.[5b] The results are given in Table I, which also gives the masses, the initial translational energy E_0 [in units of $m(\lambda w_0/b)^2$], the exact ΔE (same units), the ratio of ΔE_{PSS} to ΔE_{exact}, the ratio of ΔE_{ST} to ΔE_{exact}, and the case number of Kelley and Wolfsberg.[7]

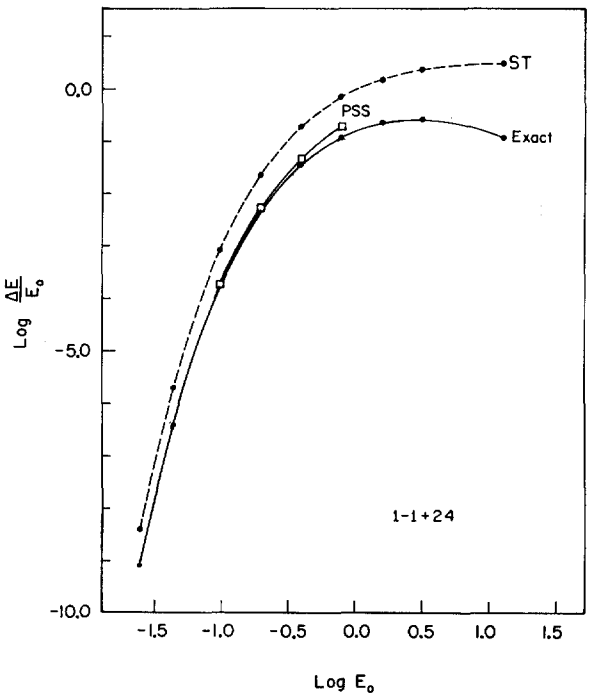

FIG. 2. Log $\Delta E/E_0$ vs log E_0 for a $1-1+24$ collision. The exact results are taken from Ref. 7.

J^0 is zero for the calculations presented in Table I. The results for several mass ratios are illustrated in Figs. 1–3. In Fig. 3, several exact KW points[7] for the $12-1+13$ case and many others of Secrest[11] are compared with the ST and PSS results.[16]

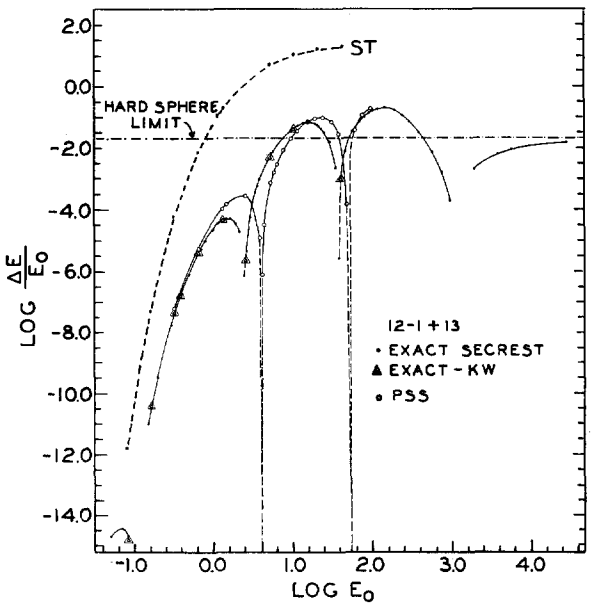

FIG. 3. Log $\Delta E/E_0$ vs log E_0 for a $12-1+13$ collision.

[16] (a) Details of the evaluation of the integrals are given in M. Attermeyer, Ph.D. thesis, University of Illinois, 1969. (b) Although most of the reported ΔE^{PSS}'s were obtained by the method in Ref. 16(a), it has been replaced by a much more rapid computation involving numerical solution of corresponding differential equations. For consistency the $\dot{\omega}$ term was omitted.

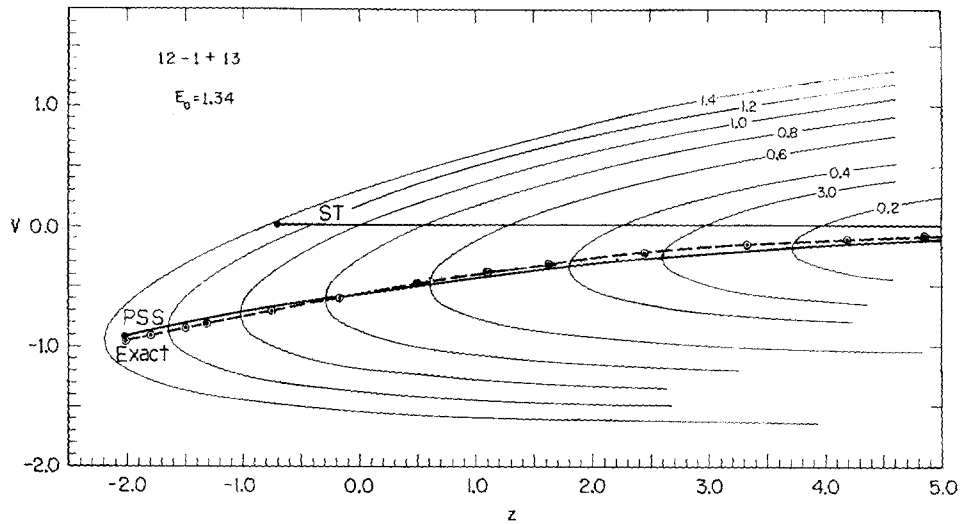

FIG. 4. Exact and approximate trajectories for a $12-1+13$ collision at $E_0=1.34$. The $v=0$ and $v_e(z)$ zeroth-order lines are indicated by ST and PSS, respectively. Exact results are indicated for negative p_z by $---$ and for positive p_z by $\odot$. Potential-energy contours are sketched in the background.

If the diatomic molecules in Table I are regarded as CH, C_2, and H_2, with respective force constants of 4.5, 9.5, and 5.7 mdyn/Å, and if the usual value[16] for $1/b$ of about 0.2 Å is used, the E_0's of the first lines for each mass ratio in Table I are 1.1, 0.27, 1.1, 1.1, 0.34, and 0.27 eV, respectively. Thus, all of the E_0's used in Ref. 7 are rather high. (Low values of E_0 frequently give rise to computational difficulties.) However, except for the $12-1+13$ case the error ratios in Table I are relatively energy independent, at least in the range investigated. Nevertheless, exact results at lower E_0's would be desirable for comparison with data on energy transfer at thermal energies.

DISCUSSION

At the lowest energy, where the near-adiabatic approximation should work best, the PSS results are very good indeed, being in error by $\approx 1\%$, 0%, 15%, 16%, 10%, and 9% at the successive mass ratios in Table I. The corresponding errors for the ST approximation are 1%, 7%, 12%, 134%, 426%, and 126 000%. The advantage of the PSS method begins to occur at a μ of 1.4 ($12-12+24$). When the ST approximation is comparable in accuracy (or, in the case of high energies for $\mu=3.6$ and 1.4, is more accurate), it is preferable to the PSS one since its integral can be evaluated analytically.

In the $12-1+13$ case, the $\log(\Delta E/E_0)$ vs $\log E_0$ plot of Fig. 3 shows the nonmonotonic behavior studied in detail by Secrest.[11] The PSS curve shows a similar behavior, somewhat shifted in phase, but the ST curve is monotonic.

Some insight into the above results is obtained from a consideration of the potential-energy surfaces, the exact trajectories, and the time evolution of the vibrational action integral given by Eq. (11). In mass-weighted space [(v, z) space] the potential-energy surface has a well-defined curved ascending gulley when μ is small, e.g., as in the $12-1+13$ case (Fig. 4) or in the $1-1+24$ case (Fig. 5). The $v_e(z)$ path defined by Eq. (8) is the zeroth-order (elastic) approximation to the trajectory for the collision in the PSS approximation and is given in Figs. 4 and 5 together with the exact trajectory for a particular E_0. The corresponding path in the zeroth-order (elastic) approximation for the ST case is the straight line $v(z)=0$. The reason for the considerable improvement of the PSS over the ST approximation for these mass ratios becomes clear.

For the $12-12+2$ mass ratio the mass-weighted surface shows a very different behavior, i.e., relatively unchannelled, at small separation distances (Fig. 6).

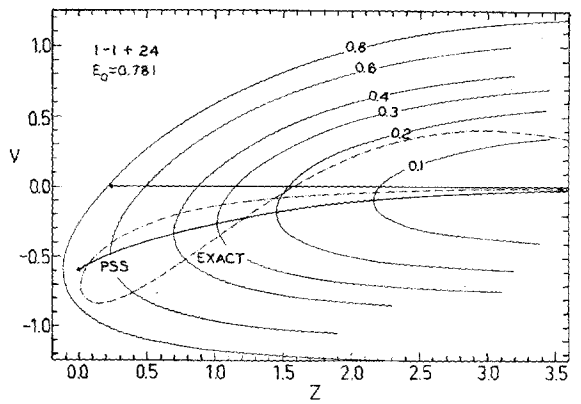

FIG. 5. Exact and approximate trajectories for a $1-1+24$ collision at $E_0=0.781$.

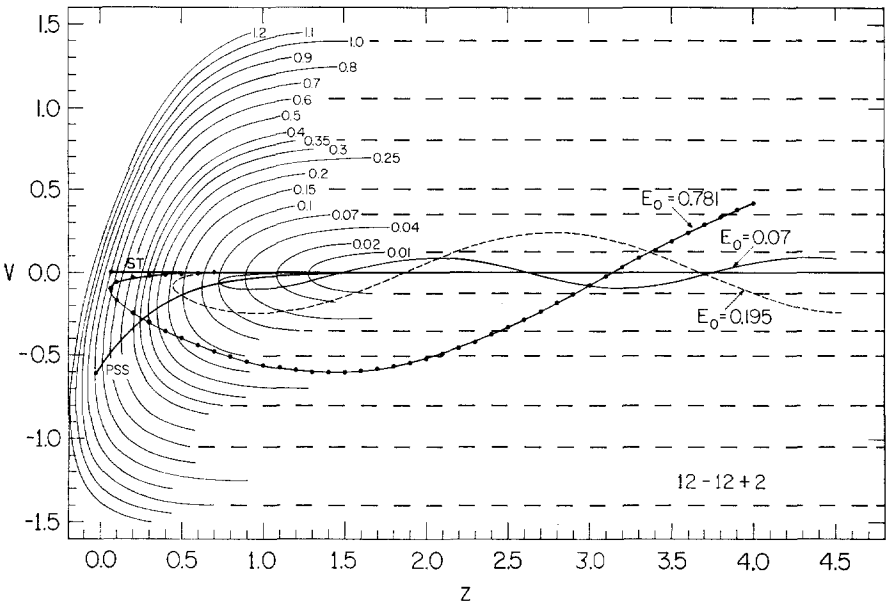

FIG. 6. Exact approximate trajectories for a 12−12+2 collision at E_0=0.781 (●) 0.195 (- - -) and 0.07 (—). The v=0 and $v_e(z)$ zeroth-order curves are indicated by ST and PSS.

In their approaching portion the exact trajectories for various E_0's are seen to agree better with the zeroth-order ST path (v=0) than with the zeroth-order PSS path [$v=v_e(z)$]. It is not surprising therefore that ST is better than PSS at high energies for this mass ratio.

The above behavior can also be understood from several other viewpoints. In the 1−1+24 and 12−1+13 collisions, if the initial relative kinetic energy is not too large, the central atom has time to adjust adiabatically to the incoming atom. In the 12−12+2 collision, it does not since the light 2 atom darts in and out, creating an impulsive force, thereby making ideal conditions for an ST approximation. In terms of the v, z coordinates, the exp $(-\mu z)$ term at large μ causes a much stronger impulsive force at small distances of separation, z, than it does (for the same z) when μ is small.

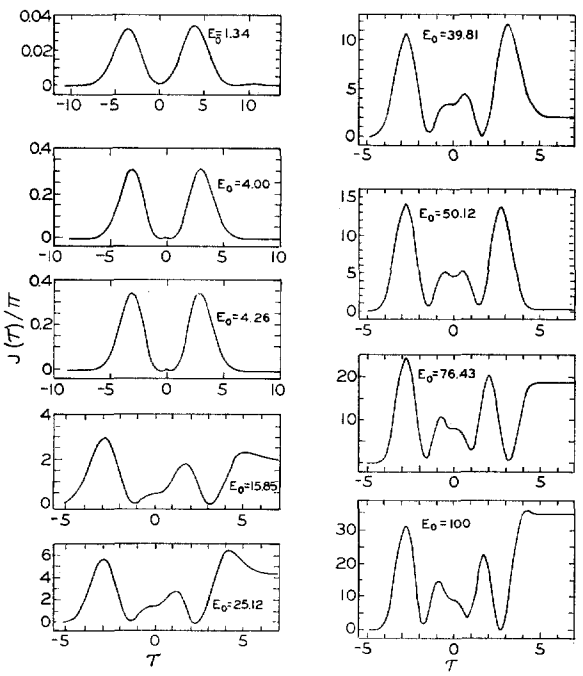

FIG. 7. Time evolution of $J(\tau)$ for various (increasing) E_0, for a 1−12+13 collision.

The nonmonotonic behavior in Fig. 3 may be understood in terms of the behavior of the vibrational action integral as follows: In Fig. 7 as E_0 increases, $J(\tau)$, given by Eq. (11), undergoes an increasing number of oscillations with the result that the final $J(\infty)$ is small for some E_0 and large for others, thereby yielding the nonmonotonic behavior in Fig. 3. An alternative explanation could be offered on the basis of a multiple-collision hypothesis[11]: In the case of hard spheres for the μ of Fig. 3 Secrest[11] has shown that there are five (intermittent) instants of contact between the colliding species. At very low E_0, to be sure, the hard-sphere analogy becomes less suitable since it is in error there by twelve orders of magnitude (Fig. 3), while the PSS method is very good.

In using Eq. (91) of Ref. 9(c) to obtain (11) rectangular (v, z) coordinates were used instead of the more general curvilinear ones and the $\dot{\omega}$ term was neglected. Further, terms higher than $(v-v_e)^2$ were omitted in (7). One or more of these approximations may account for the displacement in phase of the exact and PSS curves in Fig. 3.[17] For example, the exact trajectory is seen in Fig. 8 to agree well with the curvilinear

[17] Recent calculations[16b] including the $\dot{\omega}$ term show that it alone does not account for the phase difference, but rather shifts the curve near log E_0=0.6 in Fig. 3 slightly to the right. The $\dot{\omega}$ term has a negligible effect at small E_0, e.g., at log $E_0=-0.5$.

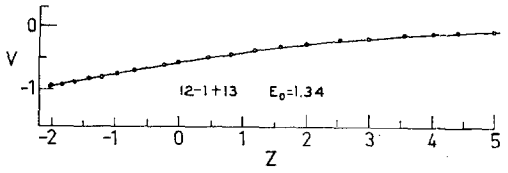

FIG. 8. Exact and curvilinear coordinate[9b] trajectories for a 12−1+13 collision at $E_0=1.34$. (Compare Fig. 4.)

reaction coordinate of Ref. 9(a). Comparison with the lesser agreement of this exact trajectory with the PSS path in Fig. 4 suggests that the curvilinear coordinate in Fig. 8 should be useful for a zeroth-order approximation in a near-adiabatic calculation[9b] at this μ.

In the light of the results in Table I we now examine some recent quantum and semiclassical calculations. For the zeroth-order (elastic) collision the Jackson–Mott distorted-wave calculation assumes the potential energy for translational motion to be that in which the oscillator coordinate has its equilibrium value.[18] Such an approximation is indeed an ST one. Mies[6] removed it by computing the actual matrix elements V_{nn}, thus converting the Jackson–Mott treatment into a true first-order distorted wave calculation. According to the results in Table I, this correction to the Jackson–Mott expression should have little effect at large μ, but a large effect at small μ. Such is indeed the case in Roberts' recent comparison[19] of exact results with those obtained from the approximate distorted wave calculated by Jackson and Mott and from (Mies') distorted wave calculations (μ ranged from 0.9 to 2.24). At sufficiently low μ the distortion may be too large for these first-order treatments, and a comparison with exact results at $\mu=0.4$ would be useful. (A first-order PSS treatment should be appropriate at low E_0, according to Fig. 3.)

The first-order distorted wave calculations become inapplicable when jumps via virtual states become important during the collision. Existing semiclassical[4] and distorted wave[2b] calculations which are infinite order with respect to the internal states allow for these virtual effects. Each of these infinite-order calculations is of the ST type, since each has (in the elastic collision) the ST type of potential energy described earlier, and so would be expected to be reasonable at large μ and poor at small μ. It is of interest in this connection to note that the infinite-order distorted wave approximation of Thiele and Weare was compared[2b] with the exact[20] results only at a large μ (3.6), and comparison at lower μ would be desirable.

[18] The exponential in (2) was expanded in powers of λy and powers higher than the first neglected. In the matrix elements V_{nn} of V over the nth oscillator wavefunction the mean of λy vanished, making all $V_{nn}=D\exp[-b(x-\lambda r_e)]$.

[19] R. E. Roberts, J. Chem. Phys. 49, 2880 (1968); cf. D. Secrest *ibid.* 49, 2880 (1968).

[20] D. Secrest and B. R. Johnson, J. Chem. Phys. 45, 4566 (1966). Our μ equals their $m^{-1/2}$.

ACKNOWLEDGMENT

The authors are deeply indebted to Professor Don Secrest of this department for many helpful discussions and for permitting us to use his exact results in advance of publication.

APPENDIX: DERIVATION OF EQ. (11)

The derivation of (11), given in Ref. 9(c), is outlined below.

The present Hamiltonian is given by (3), plus the approximation embodied in (6). If, at each z, the local vibrational v motion is treated as "adiabatic" the local vibrational energy

$$[(p_v^2/2)+U(v,z)-U(v_e,z)]$$

has its adiabatic value. The latter depends only on z and on the (initial) vibrational action J_0, and is denoted by $E_{\rm vib}(J_0,z)$. The z motion then satisfies the following equation, obtained from (3):

$$\tfrac{1}{2}\dot{z}^2+U(v_e,z)=E-E_{\rm vib}(J_0,z). \qquad \text{(A1)}$$

This equation is solved for $z(t)$, after first determining $E_{\rm vib}(J_0,z)$. The latter can be determined from the expression for J_0.[21]

Because the zeroth-order approximation is an adiabatic one, the calculation of higher approximations, i.e., the calculation of nonadiabatic corrections, can be performed by transforming from (v,p_v) to local vibrational action-angle variables (J,w). This transformation can be introduced via a generating function[22] $W^*(v,w,z)$ given later:

$$J=\partial W^*/\partial w, \qquad p_v=\partial W^*/\partial v. \qquad \text{(A2)}$$

The equations of motion then become

$$\dot{J}=-\partial\bar{H}/\partial w, \qquad \dot{w}=\partial\bar{H}/\partial J, \qquad \text{(A3)}$$

where

$$\bar{H}(J,w,t)=H(v,p_v)+\partial W^*(v,w,z)/\partial t. \qquad \text{(A4)}$$

In (A4) the dependence of z on t is given via (A1). The net change of J provides immediately, on integrating (A3), the net change of vibrational action and, thereby, of vibrational energy. (In the case of a locally harmonic oscillator the local vibrational energy is $J\omega/2\pi$.) W^* for a locally harmonic oscillator is[22]

$$W^*(v,w,z)=\tfrac{1}{2}\omega(v-v_e)^2\cot 2\pi w, \qquad \text{(A5)}$$

where v_e is $v_e(z)$ and where z denotes $z(t)$, obtained from solution of Eq. (A1) for the z motion. From

[21] The definition of J_0,

$$J_0=\oint p_v dv=\oint\{2(E_{\rm vib}-[U(v,z)-U(v_e,z)])\}^{1/2}dv,$$

is employed. When (6) is introduced for $U(v,z)$, integration yields $J_0=E_{\rm vib}/(\omega/2\pi)$.

[22] H. C. Corben and P. Stehle, *Classical Mechanics* (John Wiley & Sons, Inc., New York, 1960), 2nd ed., pp. 190–191.

(A2)–(A5), one finds

$$\dot{J} = -2\dot{v}_e(\omega\pi J)^{1/2} \sin 2\pi w - (J\dot{\omega}/\omega) \cos 4\omega w, \quad \text{(A6)}$$

$$\dot{w} = (\omega/2\pi) - \tfrac{1}{2}\dot{v}_e(\omega/J\pi)^{1/2} \cos 2\pi w + (\dot{\omega}/4\pi\omega) \sin 4\pi w. \quad \text{(A7)}$$

The reasoning in Ref. 9(c) [used to obtain (93) from (86) and (87)] is next employed to integrate (A6) and (A7) approximately, thus yielding (11), when the $\dot{\omega}$ terms are omitted. Inclusion of the $\dot{\omega}$ terms adds, in one approximation, as it did in Ref. 9(c), an additional term, Δ:

$$\Delta = -J^0 \int_{-\infty}^{t} \left(\frac{\dot{\omega}}{\omega}\right) \cos 2\left(\int_{\tau_0}^{\tau'} \omega dt'' + \delta\right) d\tau' \quad \text{(A8)}$$

to Eq. (11).

THE JOURNAL OF CHEMICAL PHYSICS VOLUME 52, NUMBER 1 1 JANUARY 1970

Resonance Raman Effect and Resonance Fluorescence in Halogen Gases*

W. Holzer,† W. F. Murphy, and H. J. Bernstein
Division of Chemistry, National Research Council of Canada, Ottawa, Canada

(Received 28 August 1969)

The various output frequencies of the argon ion laser at 5145, 5017, 4965, 4880, and 4765 Å lie in the absorption bands of the heavier halogen gases. With the appropriate choice of exciting line, either resonance Raman effect or resonance fluorescence can be observed. The difference between the two types of spectra are discussed in some detail. In the case of a strong resonance Raman effect, overtone sequences up to the 14th harmonic could be observed. Raman frequencies, depolarization ratios, and relative scattering cross sections are given for the fundamentals and overtones of Cl_2, Br_2, I_2, BrCl, ICl, and IBr at 4880 Å excitation.

I. INTRODUCTION

Fluorescence spectra and the Raman effect can be observed using similar experimental techniques. The resonance fluorescence of gases has been studied in detail[1] but "prelaser" gas-phase Raman spectroscopy[2,3] was restricted to transparent gases. Thus there are no experimental gas-phase Raman data available concerning cases in which excitation occurs close to or within absorption bands. This region has been investigated in the liquid and solid phase[4] and is usually referred to as "resonance Raman effect." Due to the rotation vibration fine structure of the absorption bands of gases, one might expect more complicated resonance effects. It is of interest to study these resonance effects and whether their properties could be categorized. The colored halogen gases provide a convenient series of compounds to investigate in this regard. Their spectroscopic constants have been, in general, accurately determined to provide a good basis for this study. The argon-ion laser is a convenient source for this experiment since these gases absorb in the vicinity of 5000 Å.

II. EXPERIMENTAL

The Raman and fluorescence spectra were excited with an argon-ion laser (Spectra Physics Model 140) at 5145, 5017, 4965, 4880, and 4765 Å. The power ranged from 1000 mW at 4880 Å to 50 mW at 5017 Å. The spectra were recorded with a Spex double monochromator, an EMI 6256 photomultiplier, and photon counting detection. The laser beam was focused into a small single-pass quartz gas cell with a $f=38$-mm lens. The beam was kept as close as 1 mm to the sample cell window, to minimize self-absorption of the Raman light. All measurements were made with the direction of observation perpendicular to the laser polarization. Depolarization ratios (ρ_S) were determined by analyzing the scattered light in front of the spectrograph slit. The depolarization ratios as well as all intensity data were derived from area measurements. Intensity data were also corrected for the spectral sensitivity of the spectrometer and detection system. The sensitivity was determined with a calibrated tungsten-band lamp. The spectral slitwidth was 7.5 cm^{-1} for intensity and depolarization measurements and 2.5 cm^{-1} for frequency measurements. The plasma lines of a He–Ne laser were used as a wavelength standard for more accurate frequency determination of the bands.

The sources for the gases were as follows: Cl_2, 99.5%, Matheson of Canada Ltd.; I_2 and Br_2, Analytical Analar reagent, British Drug Houses; IBr and ICl, Fisher Laboratory Chemical purified. The gas BrCl was prepared by mixing Br_2 with an excess of Cl_2.

* Issued as NRCC No. 11016.

† National Research Council of Canada Postdoctoral Fellow 1967–1969.

[1] P. Pringsheim, *Fluorescence and Phosphorescence* (Interscience Publishers, Inc., New York, 1949).

[2] B. P. Stoicheff, *Advances in Spectroscopy* (Interscience Publishers, Inc., New York, 1959), Vol. 1, p. 91.

[3] W. F. Murphy, W. Holzer, and H. J. Bernstein, Appl. Spectry. **23**, 211 (1969).

[4] J. Behringer in *Raman Spectroscopy*, H. A. Szymanski, Ed. (Plenum Press, Inc., New York, 1967), p. 168.